Check for updates

Transition from viscoelastic to fracture-like peeling of pressure-sensitive adhesives†

Marion Grzelka, [ID] *[a] Stefan Kooij, [ID] [a] Sander Woutersen, [ID] [b] Mokhtar Adda-Bedia [ID] [c] and Daniel Bonn [ID] [a]

We investigate the process of the slow unrolling of a roll of typical pressure-sensitive adhesive, Scotch tape, under its own weight. Probing the peeling velocities down to nm s^{-1} resolution, which is three orders of magnitudes lower than earlier measurements, we find that the speed is still non-zero. Moreover, the velocity is correlated to the relative humidity. A humidity increase leads to water uptake, making the adhesive weaker and easier to peel. At very low humidity, the adhesive becomes so stiff that it mainly responds elastically, leading to a peeling process akin to interfacial fracture. We provide a quantitative understanding of the peeling velocity in the two regimes.

1 Introduction

Adhesion is important for many everyday engineering and biological processes, but it remains ill-understood at a fundamental level. Different adhesion mechanisms, such as mechanical interlocking and electrostatic, chemical and van der Waals bonding, have all been proposed.[1] However there is no unified theory for adhesion, and many adhesion mechanisms are believed to be specific to particular material combinations. In addition, adhesion forces can depend very sensitively on the specific geometry of the debonding, with the peeling force differing by orders of magnitude for the same adhesion energy.[1] This makes it notoriously difficult to predict the adhesion behavior. One of the key examples here is pressure sensitive adhesives (PSAs) that are typically used in adhesive tape and sticky notes.[2] In spite of the fact that these are materials that are used by many people every day, there is no fundamental understanding of the adhesive strength and consequently the force necessary to undo the adhesive bond.[3]

In this paper we provide such an understanding for the unsticking of PSAs under different environmental conditions.

In these and many other adhesive systems the adhesive is typically 'soft', *i.e.*, visco-elastic,[4,5,6,7] and this turns out to provide the key to a quantitative understanding. Most of us have experienced sticking the end of a piece of scotch tape to the edge of a table or desk, while using a freshly cut bit from the roll. The generic observation is that the tape stuck to the table does not appear to unroll under the weight of the roll. Contrary to this idea, we show here that at long timescales the tape does in fact start to unroll right away, with a speed scaling with the force, *i.e.*, the weight of the remaining tape on the roll. We find that the adhesive properties depend strongly on the environment, notably on the humidity, with a very strong dependence of the peeling speed on the environmental humidity. At very low humidity, the PSA becomes very rigid and exhibits a solid-like elastic behavior. In this second regime, we suggest that the unsticking is due to an interfacial fracture that propagates with a speed that depends on the fracture energy.

2 Methods and results

The studied tape (3M 810 Magic Scotch) is a PSA composed of a synthetic acrylic adhesive layer of thickness e = 28 μm, and a 38 μm-thick matte cellulose acetate backing. To investigate the ease with which this tape can be peeled from itself, we first study the unrolling of a suspended roll of tape of approximately 21 g under the action of gravity over a period of one month. The changing mass of the roll of tape is less than 1.3 g over a month, leading to a change of 6% on the applied force: we neglected this change in further discussion. The time of flight of a laser pulse is used to measure the vertical distance from the roll of tape to a reference point (see Fig. 1(a)). The setup is surrounded by a metal casing to prevent any airflow from

[a] *van der Waals-Zeeman Institute, Institute of Physics, University of Amsterdam, Amsterdam 1098XH, The Netherlands. E-mail: m.grzelka@uva.nl*

[b] *Van't Hoff Institute for Molecular Science, University of Amsterdam, Amsterdam 1098XH, The Netherlands*

[c] *Université de Lyon, Ecole Normale Supérieure de Lyon, Université Claude Bernard, CNRS, Laboratoire de Physique, Lyon F-69342, France*
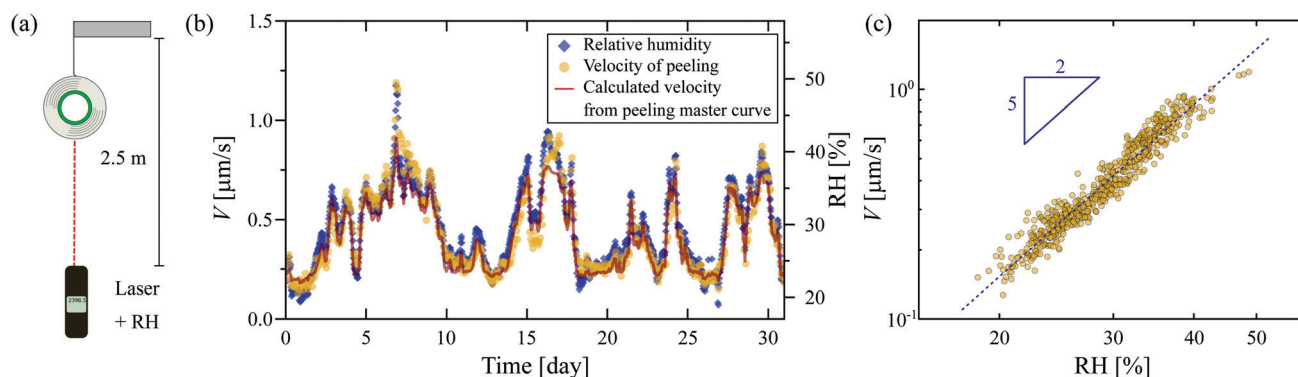
Fig. 1 Unrolling of a suspended roll of tape over a period of one month. (a) Illustration of the set-up. A roll of Scotch tape ($m \approx 21$ g) is suspended 2.5 m above a reference point, with the exact distance measured as a function of time using a laser distance meter. Temperature and relative humidity (RH) are monitored throughout the experiments. (b) Both the downward velocity V of the roll of tape and the relative humidity RH fluctuate strongly with time. The red line is the velocity of peeling calculated using the time–humidity superposition principle. (c) Peeling velocity, as extracted from (b), as a function of relative humidity. The dotted line shows a fitted power law of exponent 5/2.

disturbing the tape roll. However, the casing is not isolated from fluctuating atmospheric conditions of the laboratory. Throughout the experiments, we monitor the relative humidity, RH, and temperature (Testo 560).

The peeling velocity V of the tape displays large fluctuations over the measurement period (Fig. 1(b)) that are strongly correlated with the variation in the relative humidity (RH), with a higher RH resulting in faster peeling of the tape. A close inspection of the time-dependencies of V and RH reveals that changes in V are delayed by roughly one hour with respect to changes in the RH, suggesting a time-dependent water uptake by the hygroscopic adhesive layer. Note that the fluctuations in RH over this timescale are negligible ($<1.7\%$). Quantitatively, Fig. 1(c) shows that the velocity scales as a power law with the RH with an exponent of 5/2: the higher the RH, the lower the resistance of the PSA, leading in turn to faster unrolling of the tape.

Next, we investigate the effect of the peeling force. In addition to the peeling of the roll of tape, where we attach different weights to the suspended roll, we also tape two layers

of the adhesive over each other on a glass plate and peel the upper layer away from the lower layer using a controlled force, mimicking what happens during the unrolling of a roll of Scotch tape. The peeling velocity is measured by tracking the peeling front using a CCD camera (Nikon D850 equipped with a macro-lens Laowa 25 mm 1 : 2.8 and Phantom Miro M310 high-speed camera with a macro-lens Sigma 105 mm 1 : 2.8), both for the roll and the two layers. The peeling of the two layers allows us to study the peeling process at the debonding region in more detail, in addition to determining the Young's modulus of the backing of the tape (see Fig. S1–S3, ESI†). Both set-ups are placed in a sealed box through which a mixture of compressed air and water vapor is flowing; varying the relative proportions allows a constant RH to be maintained in the range of 1.9–98%. The temperature is kept constant at 20 ± 0.5 °C. The highest applied force of 1.27 N is chosen to avoid stick-slip effects: we focus on the steady-state regime of peeling for a low peeling velocity ($V < 10$ μm s^{-1}). It is customary to discuss the peeling speed as a function of the strain energy release rate G, which is directly linked to the applied load F through the Rivlin
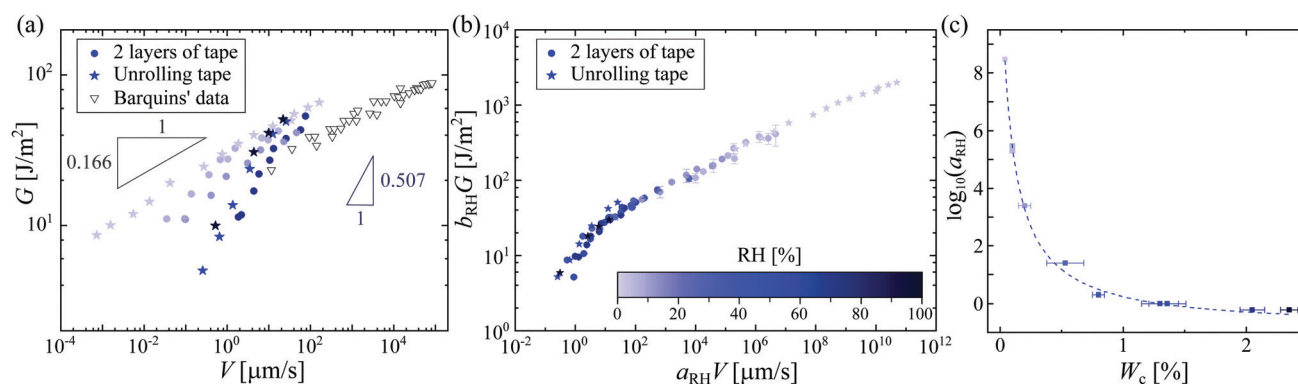

Fig. 2 (a) Strain energy release rate G as a function of peeling velocity V of the adhesive for a suspended unrolling roll of tape (stars) and two layers of tape on glass (filled circles). The color scale (same as in (b)) indicates the different relative humidities. For comparison, we plot Barquins' data[13] for the peeling of Scotch 3M 600. (b) Peeling master curve with RH$_{ref}$ = 56.7%. The rescaled strain energy release rate $b_{RH}\cdot G$ (with b_{RH} = RH$_{ref}$/RH) is plotted against the rescaled peeling velocity $a_{RH}\cdot V$. The master curve is built using the data reported in Fig. S4 (ESI†). (c) Logarithm of the rescaling factor a_{RH} as a function of the water content W_c in the adhesive tape. The dashed line is the best fit with eqn (1), following the concept of 'time–humidity' superposition.

equation,[8] $G = F(1 - \cos\theta)/b$, where $b = 19$ mm is the tape width and $\theta \approx \pi/2$ is the peeling angle in our experiment (see Fig. S1, ESI†).

As usually found in the literature, we plotted in Fig. 2(a) the energy release rate G as a function of the velocity of peeling V on a log–log scale; note that we are able to determine the velocity of the tape roll down to ~nm s^{-1} – it is therefore not surprising that one does not observe the unpeeling of roll of tape that is stuck on a desk. At a fixed RH, it is tempting to interpret our data with the extensively used[9,10,11] but hitherto unexplained power-law behavior of Maugis and Barquins,[12] $G \propto V^n$. However, when looking at the effect of the RH, it would appear that the exponent n depends strongly on RH, varying from 0.166 ± 0.003 at RH = 1.9% up to 0.507 ± 0.031 at RH = 98%. This means that for small applied forces, a humid environment boosts the peeling velocity by four orders of magnitude. The strong dependence of the exponent on the RH is not completely understood. Moreover, a second mystery arises for these simple experiments: at low RH, we find an exponent close to the very small value of $n \approx 1/8$ that was found by Barquins for a different adhesive tape.[13] In the following, we focus our discussion on understanding the effect of the humidity on the peeling and then try to understand this small exponent for low RH.

3 Discussion

The minimal peeling energies measured in the present work at the low peeling velocities are about 4 J m^{-2}, which are still much higher than the Dupré interfacial work of adhesion for typical adhesive interfaces, which is around 0.1 J m^{-2}.[3] Thus, there must be a source of visco-elastic dissipation in the peeling dynamics. As the Young's modulus of the backing of the tape is found to be almost independent of RH, $\langle E_{back}\rangle = 1.44 \pm 0.26$ GPa (see Fig. S3, ESI†), such differences in the peeling within a dry and a humid environment must be due to important changes in the adhesive material itself. Contrary to the effect of humidity, the effect of temperature on the peeling of adhesives has been widely studied.[4,5,6,14] Gent et al.[5] and Kaelble[4] were among the first to show that increasing the temperature leads to a smaller dissipation in the adhesive, and hence a larger peeling speed for a given force. They proposed a scaling procedure to collapse all temperature-dependent peeling curves onto a single master curve, following the same approach as the time–temperature superposition (TTS) principle in polymer rheology.[15] The peeling measurements for different temperatures are then rescaled in time using a coefficient $a_T(T)$, comparable to the rheological factor in the TTS principle, to create a master curve that collapses around the data for a reference temperature T_{ref}, which is usually chosen as the ambient temperature. The dependence of a_T on temperature follows the Williams–Landel–Ferry prediction for polymer liquids.[14] The parameter a_T reflects the molecular mobility of the polymer chains: the higher a_T, the less mobile are the chains.[15]

Our observations here are very similar, but are as a function of humidity rather than temperature; we therefore propose the construction of a peeling master curve for different relative humidities. Rescaling the peeling velocity by a factor $a_{RH}(RH)$ and the strain energy release rate G by $b_{RH} = RH_{ref}/RH$ with RH_{ref} being the reference relative humidity, we build the master curve with a reference data set for $RH_{ref} = 56.7\%$, such that $a_{RH}(56.7\%) = 1$. This peeling master curve is plotted in Fig. 2(b), based on the data presented in Fig. S4 (ESI†). As in the construction of the rheology master curve,[15] the rescaling factor $a_{RH}(RH)$ is manually tuned to obtain this peeling master curve (Fig. S5, ESI†). We find that a_{RH} varies over 9 orders of magnitude, similarly as was reported in the time–humidity rheology of different polymers.[16,17,18] The factor a_{RH} has the same physical meaning as a_T: a high value of a_{RH} means less mobile polymer chains in the adhesive.

In order to connect the RH to the adhesion characteristics of the Scotch tape material, we apply the concept of 'time–humidity' superposition[18,19,20] to the dependence of a_{RH} with the water content W_c absorbed by the hygroscopic adhesive:

$$\log_{10}(a_{RH}) = \frac{-D_1(W_c - W_{c,ref})}{D_2 + W_c - W_{c,ref}}, \tag{1}$$

where $W_{c,ref}$ is the water content of the adhesive at RH_{ref} and D_1 and D_2 are empirical constants. This means that a lower water content leads to a higher value of a_{RH}: the polymer chains are less mobile when the amount of absorbed water is low. The amount of water is measured as a function of RH using a simple gravimetric test (Fig. S6, ESI†). The dashed line in Fig. 2(c) is the best fit to eqn (1), with $D_1 = 0.87 \pm 0.05$, $D_2 = 1.39 \pm 0.01\%$, and $W_{c,ref} = 1.30\%$ for $RH_{ref} = 56.7\%$. The values of D_1 and D_2 are in good agreement with known constants for different polymers.[18,19] This shows that the rescaling factor a_{RH} of the peeling master curve is indeed linked to changes in the visco-elastic behavior of the adhesive. Following the analogy with the TTS principle, one possible mechanism to explain the dependence of a_{RH} on the water content in the PSA is the hydroplastization of the adhesive: when the water content increases, the glass transition temperature T_g of the adhesive decreases.[20,21] Even though no direct measurement of the glass transition temperature was performed on our tape, such hydroplastization of acrylic adhesive has already been reported in the literature:[22] Bianchi et al. reported a decrease of the T_g between 10 and 40 °C. A similar trend is highly possible in the tape we used for our experiments. At low RH the glass transition temperature would be closer to the ambient temperature than at high RH. Thus, the polymer chains in the adhesive are less mobile in the adhesive at low humidity: the adhesive is closer to the glass transition point at low RH and thus responds more elastically, and, respectively, the viscous effects dominate at high RH.

Another way to estimate the visco-elasticity of the adhesive is to calculate the Deborah number: for high Deborah numbers, elasticity dominates, whereas viscous effects become important for small Deborah numbers. Following the analogy with the

TTS principle,[23] it is possible to estimate the Deborah number De for our peeling experiments:

$$De = \tau_d a_{RH} V/e \qquad (2)$$

where τ_d is the terminal relaxation time and e is the thickness of the adhesive layer. Here, τ_d is estimated from values of the literature[23] as no dynamic mechanical analysis was performed on the Scotch tape 810. By evaluating $\tau_D \approx 1000$ s, the Deborah number De would be in the range 10^1–10^{12}: the adhesive is more elastic at low RH and more viscous at high RH. Note that a lower estimated value for the terminal relaxation time ($\tau_D < 100$ s) would even lead the Deborah number being below 1, meaning the the Scotch tape would behave as a 'liquid-like' system and flow.

Finally, to support the robustness of our approach, we calculated the evolution of the velocity of peeling $V(t)$ for the unrolling of the tape followed over a month (Fig. 1) based on the measurement RH(t) (see details in the ESI†). We show in Fig. 1(b) the the calculated $V(t)$ indeed collapses with the experimental data. To summarize, the high impact of the relative humidity on the peeling of Scotch tape is due to changes in the bulk visco-elastic properties of the adhesive. The hydroplastization of the adhesive then gives a satisfactory explanation for the dependence of the peeling velocity on the relative humidity: the higher the RH, the more easily the adhesive is peeled.

It is then tempting to attribute the very low exponent $n = 0.166$ at RH = 1.9% presented in Fig. 2(a) to the hydroplastization of the adhesive. However, this exponent is surprisingly close to the one found by Barquins ($n = 0.146$)[13] where they did not monitor the RH for their experiments. The IR characterization of the tape 3M 600 they used presents no trace of water (see Fig. S7, ESI†): the time–humidity superposition principle is not applicable for their experiments. Bulk viscoelastic dissipation is not the main peeling mechanism there. Chopin *et al.*[7,11] recently proposed an explanation for such a low exponent by taking into account the non-linear rheology of the stretched fibrils. Within the resolution of our experiments, the stretching of fibrils is rate independent (see Fig. S11, ESI†): the adhesion curve $G(V)$ is dominated by the linear viscoelasticity of the adhesive and not the non-linear rheology of the fibrils. Here, we rather propose to take into account interfacial dissipation. These peeling experiments are close to the limit in which the adhesive behaves elastically. Therefore, in order to detach, a fracture has to propagate within the adhesive or between the adhesive and the backing. To rationalize the rate-dependence of the fracture energy of elastomers, Chaudhury *et al.* proposed a fracture mechanism based on the kinetic theory of bond rupture.[24,25,26] According to Evans,[27] when a polymer chain is stretched with a force f, its activation energy of dissociation decreases by $f\lambda$, where λ is the activation length of a bond, usually approximated to the length of a chemical bond ($\lambda \approx 0.1$ nm).[24] This allows quantification of how the probability of failure of any bond in the polymer chain varies with the applied force. Chaudhury's model
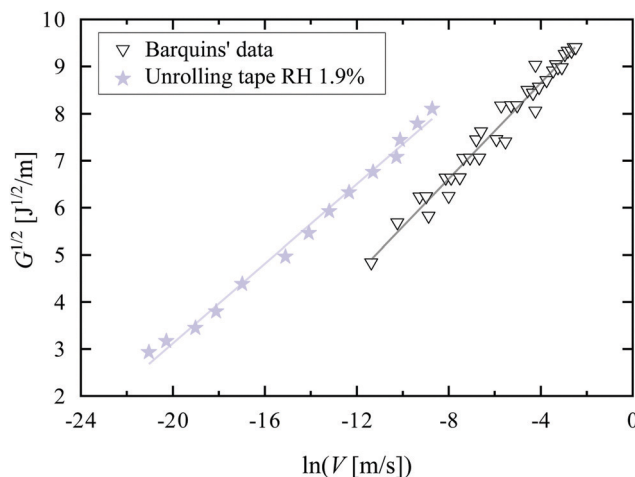

Fig. 3 Square root of the strain energy release rate G as a function of the logarithm of the peeling velocity V for the unrolling tape roll at RH = 1.9% (stars) and Barquins' data[13] (triangles). For our experiments, we assume the stretching velocity of a bond $V_{stretch}$ to be equal to the peeling velocity V. The solid lines are fits to eqn (3).

proposes the strain energy release rate G to depend on the stretching velocity of a bond $V_{stretch}$ as:

$$G = \left(\frac{\Sigma_0}{2k_s}\right)\left[\left(\frac{k_B T}{\lambda}\right)\ln\left(\frac{k_s \lambda \tau_- V_{stretch}}{n_{bond} k_B T}\right)\right]^2, \qquad (3)$$

where k_B is the Boltzmann constant, T is the temperature, n_{bond} is the number of bonds per polymer chain, Σ_0 is the number of load-bearing polymer chains per unit area, k_s is the stiffness of the polymer chain, and τ_- is the characteristic time of bond dissociation.

In Fig. 3, we plot $G^{1/2}$ as a function of $\ln(V)$ for our tape at RH = 1.9% and for Barquins' data.[13] Chaudhury's model describes both data sets very well, explaining the small exponent: the behavior is in fact not a power-law behavior with a small exponent, but rather a logarithmic dependence due to the presence of an activated process.

From the fits, we can then obtain estimates of the spring constant k_s and the characteristic time τ_-. Assuming $n_{bond} \in [100$–$1000]$,[24,26,28] and $\Sigma_0 \approx 10^8$ chains per m²,[24,28,29] we find, respectively, $k_s = 11.6 \pm 0.6$ mN m^{-1} and τ_- between 3.4×10^4 and 3.4×10^5 s for our data and $k_s = 8.0 \pm 0.6$ mN m^{-1} and τ_- between 6.6×10^2 and 6.6×10^3 s for the data of Barquins'. Note that these stiffnesses are one order of magnitude lower than the typical stiffness of the polymer chain for a strong bond ($k_s = 0.5$ N m^{-1}), meaning that the bond in the adhesive breaks long before its full extension.[30] Furthermore, according to Eyring's model, the bond dissociation time τ_- is:

$$\tau_- = \frac{h}{k_B T}\exp\left(\frac{E_a}{k_B T}\right), \qquad (4)$$

where h is Planck's constant. Thus, the activation energy of bond dissociation $E_a = 105 \pm 3$ kJ mol^{-1} in our experiment and $E_a = 91 \pm 3$ kJ mol^{-1} for the data of Barquins'. These energies are smaller than the dissociation energy of a covalent bond
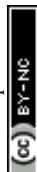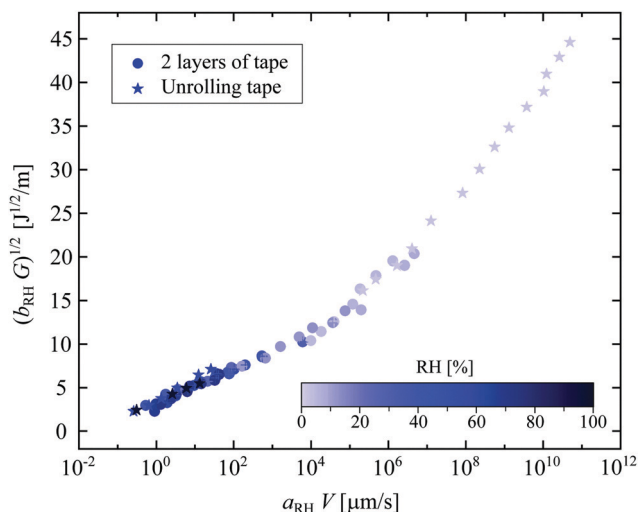
Fig. 4 Square root of the rescaled strain energy release rate $b_{RH}G$ as a function of the rescaled peeling velocity $a_{RH}V$ on a log–linear scale. This graph presents the same data as in Fig. 2(b) but plotted so that it can be compared with Chaudhury's theory.

(~ 400 kJ mol^{-1})[30] and the decomposition activation energy of an acrylic adhesive (~ 200 kJ mol^{-1}).[31] However, the activation energy of bond dissociation for our experiments and Barquins' ones are respectively of the order of $7 E_{Hbond}$ and $6 E_{Hbond}$, with the hydrogen bond dissociation $E_{Hbond} \approx 15$ kJ mol^{-1}.[29,30] Interestingly, the small differences between the two data sets can be attributed to the difference of the adhesives in the two different types of Scotch tape, which might be a useful avenue to pursue for improving pressure sensitive adhesives.

Such a fracture-like theory does not preclude any influence of visco-elasticity on the fracture behavior. For instance, viscoelastic fracture that agrees with Griffith fracture theory has been observed on much softer materials than the PSA we used.[32] Then arises the question of how to link Chaudhury's theory and the building of a peeling master curve. In Fig. 4, the data presented in the peeling master curve (Fig. 2(b)) are plotted to be compared with Chaudhury's model (see eqn (2)): the square root of the rescaled strain energy release rate $b_{RH}G$ as a function of the rescaled peeling velocity $a_{RH}V$ in a log–linear scale.

As the data follow two lines, we distinguish two regimes. We attribute the regime at 'high' humidity to a competition between the interfacial dissipation, described by Chaudhury's model, and the viscous dissipation in the adhesive. Indeed, such bulk dissipation is not taken into account in Chaudhury's model. To our knowledge, there is no complete theory that proposes a picture of the whole mechanism. Note that the limit between these two behaviors is not sharp since part of the data at RH = 7.4% follows the same trend as some at RH = 1.7%. More extensive experiments with a controlled chemistry of the adhesive would be needed to clearly distinguish the boundary between bulk dissipation, reflected with the construction of the peeling master curve, and interfacial dissipation, explained by Chaudhury's model. Probe tests might be used to quantify the adhesion and investigate further these bulk and interfacial

effects, as recently proposed by Wang et al.[33] In addition, extra theoretical efforts are desired to construct a model that can include both the bulk and interfacial dissipation.

4 Conclusion

In summary, we provided an understanding of the force necessary to peel a typical PSA depending on the environmental conditions. The first surprise is the sensitivity to the humidity: the more humid the environment, the faster the tape peels for a given force, with a power-law relationship between speed and force that can be successfully described using a master curve applying 'time–humidity' superposition. The second surprise is that for very low humidities, the adhesive becomes strongly elastic and a completely different regime emerges. Chaudhury's theory of rate-dependent bond fracture allows the observed logarithmic dependence of the peeling velocity on the strain energy release rate to be quantitatively described as an activated process, which explains also the previously reported power-law behavior with an inexplicably small exponent in this regime. This work opens the way to developing a complete quantitative understanding of soft visco-elastic adhesives by showing that, depending on the external parameters, either viscous or elastic behavior can be expected and explained.

Conflicts of interest

There are no conflicts to declare.

Acknowledgements

Notes and references

1 J. N. Israelachvili, *Intermolecular and Surface Forces*, Academic Press, 3rd edn, 2015.
2 C. Creton, *MRS Bull.*, 2003, **28**, 434–439.
3 C. Creton and M. Ciccotti, *Rep. Prog. Phys.*, 2016, **79**, 046601.
4 D. H. Kaelble, *J. Colloid Sci.*, 1964, **19**, 413–424.
5 A. N. Gent, R. P. Petrich and D. Tabor, *Proc. R. Soc. London, Ser. A*, 1969, **310**, 433–448.
6 C. Derail, A. Allal, G. Marin and P. Tordjeman, *J. Adhes.*, 1998, **68**, 203–228.
7 J. Chopin, R. Villey, D. Yarusso, E. Barthel, C. Creton and M. Ciccotti, *Macromolecules*, 2018, **51**, 8605–8610.
8 R. S. Rivlin, in *Collected Papers of R.S. Rivlin: Volume I and II*, ed. G. I. Barenblatt and D. D. Joseph, Springer, New York, NY, 1997, pp. 2611–2614.
9 M. Barquins and D. Maugis, *J. Adhes.*, 1981, **13**, 53–65.

10 A. J. Crosby and K. R. Shull, *J. Polym. Sci., Part B: Polym. Phys.*, 1999, **37**, 3455–3472.

11 R. Villey, C. Creton, P.-P. Cortet, M.-J. Dalbe, T. Jet, B. Saintyves, S. Santucci, L. Vanel, D. J. Yarusso and M. Ciccotti, *Soft Matter*, 2015, **11**, 3480–3491.

12 D. Maugis and M. Barquins, *J. Phys. D: Appl. Phys.*, 1978, **11**, 1989–2023.

13 M. Barquins and M. Ciccotti, *Int. J. Adhes. Adhes.*, 1997, **17**, 65–68.

14 G. Marin and C. Derail, *J. Adhes.*, 2006, **82**, 469–485.

15 J. D. Ferry, *Viscoelastic Properties of Polymers*, Wiley, 1961.

16 S. Onogi, K. Sasaguri, T. Adachi and S. Ogihara, *J. Polym. Sci.*, 1962, **58**, 1–17.

17 S.-M. Zhou, K. Tashiro and T. Ii, *J. Polym. Sci., Part B: Polym. Phys.*, 2001, **39**, 1638–1650.

18 V. Fabre, G. Quandalle, N. Billon and S. Cantournet, *Polymer*, 2018, **137**, 22–29.

19 A. Ishisaka and M. Kawagoe, *J. Appl. Polym. Sci.*, 2004, **93**, 560–567.

20 N. B. Hatzigrigoriou, S. N. Vouyiouka, C. Joly, P. Dole and C. D. Papaspyrides, *J. Appl. Polym. Sci.*, 2012, **125**, 2814–2823.

21 N. B. Hatzigrigoriou, C. D. Papaspyrides, C. Joly, J. Pinte and P. Dole, *Polym. Eng. Sci.*, 2011, **51**, 532–541.

22 N. Bianchi, F. Garbassi, R. Pucciariello and G. Romano, *Int. J. Adhes. Adhes.*, 1990, **10**, 19–23.

23 H. Lakrout, C. Creton, D. Ahn and K. R. Shull, *Macromolecules*, 2001, **34**, 7448–7458.

24 M. K. Chaudhury, *J. Phys. Chem. B*, 1999, **103**, 6562–6566.

25 A. Ghatak, K. Vorvolakos, H. She, D. L. Malotky and M. K. Chaudhury, *J. Phys. Chem. B*, 2000, **104**, 4018–4030.

26 C.-Y. Hui, T. Tang, Y.-Y. Lin and M. K. Chaudhury, *Langmuir*, 2004, **20**, 6052–6064.

27 E. Evans and K. Ritchie, *Biophys. J.*, 1997, **72**, 1541–1555.

28 Z. Zhu, Y. Xia, J. Li, C. Jiang and H. Jiang, *Eng. Fract. Mech.*, 2019, **222**, 106743.

29 J. Macron, B. Bresson, Y. Tran, D. Hourdet and C. Creton, *Macromolecules*, 2018, **51**, 7556–7566.

30 F. J. Cedano-Serrano, U. Sidoli, A. Synytska, Y. Tran, D. Hourdet and C. Creton, *Macromolecules*, 2019, **52**, 3852–3862.

31 Y. Wang, J. Long, Y. Bai, L. Shao and S. Qi, *J. Adhes. Sci. Technol.*, 2016, **30**, 300–312.

32 D. Bonn, H. Kellay, M. Prochnow, K. Ben-Djemiaa and J. Meunier, *Science*, 1998, **280**, 265–267.

33 Q. Wang, W. B. Griffith, M. Einsla, S. Zhang, M. L. Pacholski and K. R. Shull, *Macromolecules*, 2020, **53**, 6975–6983.